IOPscience iopscience.iop.org

Home Search Collections Journals About Contact us My IOPscience

Electronic structure and band gap of zinc spinel oxides beyond LDA: $ZnAl_2O_4$, $ZnGa_2O_4$ and $ZnIn_2O_4$

This article has been downloaded from IOPscience. Please scroll down to see the full text article.

2011 New J. Phys. 13 063002

(http://iopscience.iop.org/1367-2630/13/6/063002)

View the table of contents for this issue, or go to the journal homepage for more

Download details:
IP Address: 157.193.13.115
The article was downloaded on 02/07/2011 at 09:43

Please note that terms and conditions apply.

New Journal of Physics
The open-access journal for physics

Electronic structure and band gap of zinc spinel oxides beyond LDA: $ZnAl_2O_4$, $ZnGa_2O_4$ and $ZnIn_2O_4$

H Dixit[1,4], N Tandon[2], S Cottenier[3], R Saniz[1], D Lamoen[1], B Partoens[1], V Van Speybroeck[3] and M Waroquier[3]

[1] CMT-group and EMAT, Departement Fysica, Universiteit Antwerpen Groenenborgerlaan 171, B-2020 Antwerpen, Belgium
[2] Instituut voor Kern- en Stralingsfysica, K U Leuven Celestijnenlaan 200D, B-3001 Leuven, Belgium
[3] Center for Molecular Modeling, Ghent University Technologiepark 903, 9052 Zwijnaarde, Belgium
E-mail: Hemant.Dixit@ua.ac.be

New Journal of Physics **13** (2011) 063002 (11pp)
Received 15 February 2011
Published 1 June 2011
Online at http://www.njp.org/
doi:10.1088/1367-2630/13/6/063002

Abstract. We examine the electronic structure of the family of ternary zinc spinel oxides ZnX_2O_4 (X = Al, Ga and In). The band gap of $ZnAl_2O_4$ calculated using density functional theory (DFT) is 4.25 eV and is overestimated compared with the experimental value of 3.8–3.9 eV. The DFT band gap of $ZnGa_2O_4$ is 2.82 eV and is underestimated compared with the experimental value of 4.4–5.0 eV. Since DFT typically underestimates the band gap in the oxide system, the experimental measurements for $ZnAl_2O_4$ probably require a correction. We use two first-principles techniques capable of describing accurately the excited states of semiconductors, namely the GW approximation and the modified Becke–Johnson (MBJ) potential approximation, to calculate the band gap of ZnX_2O_4. The GW and MBJ band gaps are in good agreement with each other. In the case of $ZnAl_2O_4$, the predicted band gap values are > 6 eV, i.e. ~ 2 eV larger than the only reported experimental value. We expect future experimental work to confirm our results. Our calculations of the electron effective masses and the second band gap indicate that these compounds are very good candidates to act as transparent conducting host materials.

[4] Author to whom any correspondence should be addressed.

© IOP Publishing Ltd and Deutsche Physikalische Gesellschaft

Contents

1. Introduction **2**
2. Computational details **3**
2.1. Pseudopotentials (PPs) 3
2.2. Density-functional theory (DFT), GW and modified Becke–Johnson (MBJ) . . 4
3. Result and discussion **4**
3.1. Structural properties and electronic band structure using DFT 4
3.2. GW and MBJ band gaps 7
3.3. Formation enthalpy 9
4. Conclusions **10**
Acknowledgments **10**
References **10**

1. Introduction

Zinc alluminate ($ZnAl_2O_4$) and zinc gallate ($ZnGa_2O_4$) are wide-band-gap semiconductors with the reported band gaps of 3.8–3.9 and 4.4–5.0 eV, respectively [1]. These wide-band-gap structures are useful in photoelectronic and optical applications and are being studied as candidate materials for reflective optical coatings in aerospace applications [2, 3]. Because of their wide band gap, they have attracted much interest as possible transparent conducting oxide (TCO) materials [4, 5]. For effective material design for this purpose, a sound knowledge of the electronic properties of these materials is essential. The structural properties and electronic structure of these materials have been studied previously [5–7] within the framework of standard density functional theory (DFT) [8, 9]. But these studies were hampered by the well-known problem that within that framework the band gap of semiconductors and insulators is severely underestimated [10]. Indeed, although the structural parameters obtained within DFT are in fairly good agreement with experiment, the band gaps are not so. For instance, the calculated DFT band gap of $ZnGa_2O_4$ is 2.79 eV [6], an underestimation of 42% with respect to the experimental value. Interestingly, in the case of $ZnAl_2O_4$, the DFT band gap is found to be 4.11 eV [6], which is roughly 5% higher than the experimental value. This is in stark contrast to the common trend and has led Sampath [6] to indicate that since the band gaps in [1] were derived from reflectance measurements of powder samples, a correction due to the particle-size dependence of light scattering may be necessary. Thus, the exact band gap value of $ZnAl_2O_4$ is at present an open question.

Fortunately, at present there are first-principles techniques that have been demonstrated to be able to describe accurately the electronic structure of semiconductors and insulators. As examples first we mention the GW approximation [10] and thereafter the recently proposed modified Becke–Johnson (MBJ) potential [11, 12] approximation. Here we apply these methods to study systematically the series ZnX_2O_4, where X = Al, Ga and In are successively heavier elements from group III of the periodic table. We focus not only on predicting the real value of the fundamental band gap in these materials, but also on other key properties in TCOs, such as the second band gap (between the two lowest conduction bands) and the electron effective mass.

The GW method is a Green's function technique that involves the ejection or injection of electrons. It links the N-particle system with the $(N \pm 1)$-particle system. In this way, the GW approximation offers a strong physical basis to correlate the band energies obtained using Green's function with the experimental band gap measured using photoemission spectroscopy. Band gaps calculated by GW are observed to be much closer to the experimental values than are DFT band gaps [13]. The MBJ exchange correlation potential proposed recently by Tran and Blaha [11, 12] is a parameterized functional that recovers the local density approximation (LDA) as a limiting case. The number of parameters that were tuned by applying this method to a test set is small (only two). MBJ calculations require barely more computation time than do regular LDA calculations, and provide band gaps that are observed to be very similar to GW band gaps [11]. The GW band gaps are calculated on top of the DFT band structure at the Γ point, using a pseudopotential (PP) and a plane wave basis set. Note that we use the non-self-consistent or 'single-shot' approximation [10]. The MBJ calculations are performed with an all-electron method using an augmented plane wave + local orbital (APW + lo) basis set.

Transition metal oxides can be particularly challenging for first-principles calculations and this is the case for the GW method as well. Indeed, while there is ample evidence that the non-self-consistent GW approximation works well in combination with PPs and a plane wave basis set within DFT–LDA [14], it has been observed that it can underestimate band gaps in transition metal oxides if no special care is taken. The exchange part of the self-energy operator within the GW approximation is inadequately treated if only cation d-states are included as valence states [15]. Therefore, a 'standard' PP with only semi-core d-states is not suitable for calculating a GW band gap in transition metal oxides. For ZnO, we have found before that the 20-electron cation PP is essential for an adequate treatment of the exchange part of the self-energy within the GW approximation [16]. In this work, we also address the question of whether the complete $n = 3(4)$ shell must be included in the Ga(In) PP to obtain accurate GW results. Thus, in this paper we present the non-self-consistent GW band gap calculated with two sets of PPs. Firstly, with the 'standard' PP containing the semi-core states ($3d^{10}$, $4s^2$ for Zn, $3d^{10}$, $4s^2$, $4p^1$ for Ga and $4d^{10}$, $5s^2$, $5p^1$ for In) and then with the entire $n = 3(4)$ shell treated as valence ($3s^2$, $3p^6$, $3d^{10}$, $4s^2$ for Zn; $3s^2$, $3p^6$, $3d^{10}$, $4s^2$, $4p^1$ for Ga and $4s^2$, $4p^6$, $4d^{10}$, $5s^2$, $5p^1$ for In). We discuss how these different PPs affect the structural properties as well as the GW band gap. The accuracy of these PPs is examined by comparison with the all-electron calculations with LDA and the MBJ potential.

2. Computational details

2.1. Pseudopotentials (PPs)

We use two sets of *ab initio* norm-conserving PPs for Zn, Ga and In as defined below.

(a) The 'standard' Zn^{12+}, Ga^{13+} and In^{13+} PPs in which the semi-core 3d(4d) state is treated as valence. The inclusion of the wide d-orbital is necessary for a correct description of the structural properties by DFT for group-IIB and -IIIA elements. Hereafter this set of PPs will be referred to as PP1.

(b) The Zn^{20+}, Ga^{21+} and In^{21+} PPs generated with the entire $n = 3(4)$ shell as valence. Since the exchange energy contribution to the self-energy operator depends on the spatial overlap of atomic orbitals, the 's' and 'p' states are also included in the valence for an adequate treatment of the self-energy. It should be noted that we do not construct our Zn^{20+}, Ga^{21+} and In^{21+} PPs for

the neutral zinc and gallium (indium) atoms, but rather for the ion with the 4s(5s) and 4p(5p) states unoccupied. The cut-off radius for the Zn and Ga atoms is chosen to be 0.43 Å for 3s, 3p and 3d orbitals and 1.38 Å for 4s and 4p orbitals. For the In atom, we choose a cut-off radius of 0.52 Å for 4s, 4p and 4d orbitals and 1.2 Å for 4s and 4p orbitals. These values for the cut-off radius show the smallest transferability error for ionic configurations of Zn/Ga/In (neutral, +1 and +2), at the cost of an increased plane wave cut-off. We have used 90 Ha as the cut-off energy for plane waves, when $Zn^{20+}/Ga^{21+}/In^{21+}$ PP is used. The PP becomes harder with the inclusion of localized core orbitals in the valence. These PPs are generated with the OPIUM code (http://opium.sourceforge.net/index.html) according to the Troullier–Martins method [17] with Perdew–Zunger LDA [18]. Hereafter this set of PPs will be referred to as PP2.

2.2. Density-functional theory (DFT), GW and modified Becke–Johnson (MBJ)

The electronic structure and the quasiparticle (GW) correction to the band gap at the Γ point have been calculated using the plane wave PP code ABINIT [19–21]. For the electronic structure the plane wave cut-off is chosen using the total energy convergence criterion of 2×10^{-2} eV. The atomic positions and structural parameters have been optimized by calculating the Hellmann–Feynman forces. The stresses are minimized with the criterion of 2×10^{-5} eV Å^{-3}. We choose a $4 \times 4 \times 4$ Monkhorst–Pack [22] k-point mesh, which yields 10 k-points in the irreducible Brillouin zone.

The parameters used within ABINIT to calculate the self-energy are optimized with a convergence criterion of 0.01 eV for the band gap at Γ. We have found that for both the screening and the self-energy calculation, 600 bands are sufficient to converge the GW band gap. The dielectric matrix is calculated with the plasmon-pole model [10] and is used to calculate the screening.

All-electron calculations with the APW + lo method were performed using the WIEN2k code [25, 26]. In this method, the wave functions are expanded in spherical harmonics inside non-overlapping atomic spheres of radius R_{MT} and in plane waves in the remaining space of the unit cell (the interstitial region). The radii for the muffin tin spheres were taken as large as possible without overlap between the spheres: $R_{MT}^{Zn} = 2.0$, $R_{MT}^{Al} = 1.9$, $R_{MT}^{Ga} = 2.0$, $R_{MT}^{In} = 2.3$ and $R_{MT}^{O} = 1.6$. The maximum ℓ for the expansion of the wave function in spherical harmonics inside the spheres was taken to be $\ell_{max} = 10$. The charge density was Fourier expanded up to $G_{max} = 16$ Ry. Atomic positions were relaxed until the forces were below 0.5 mRy au^{-1}. The plane wave expansion of the wave function in the interstitial region was truncated at $K_{max} = 4.7$. A converged k-mesh of 16 k-points in the irreducible part of the Brillouin zone was used.

3. Result and discussion

3.1. Structural properties and electronic band structure using DFT

ZnX_2O_4 (X = Al, Ga and In) adopt the normal spinel structure (space group Fd-3m). They are characterized by the lattice parameter a and an internal parameter u. The Zn atoms are located at the Wyckoff positions 8a (1/8, 1/8, 1/8) tetrahedral sites, whereas Al, Ga or In atoms are located at the 16d (1/2, 1/2, 1/2) octahedral sites and the O atoms at 32e (u, u, u) of the face-centered cubic structure. It has been shown by experiment [23] as well as theory [24] that for these compounds ($ZnAl_2O_4$ and $ZnGa_2O_4$), the normal spinel structure is more favorable than

Table 1. The optimized lattice constant (in Å) and the internal coordinate (u) of three spinel compounds, calculated using either PP (PP1 and PP2; see text) or an all-electron method.

Compound	PP1	PP2	All-electron method	Experiment [23]
$ZnAl_2O_4$	7.9893	7.9849	8.0464	8.086
u	0.2642	0.2647	0.2638	0.2636
$ZnGa_2O_4$	8.2644	8.3284	8.2693	8.33
u	0.2611	0.2611	0.2612	0.2617
$ZnIn_2O_4$	8.8420	8.8790	8.9297	–
u	0.2553	0.2556	0.2558	–

the inverse spinel structure, where the tetrahedral sites are occupied by the X atoms and the octahedral sites are occupied by equal numbers of Zn and O atoms. We therefore consider only the normal spinel structure in this work. The structural properties are summarized in table 1, which shows the optimized lattice constant and 'u' parameter for both sets of PPs and for an all-electron calculation, in all cases with plain LDA. For comparison the experimental values are also listed. Experimental data are not available for $ZnIn_2O_4$. Lattice constants and internal parameters for both PPs are in good agreement with the corresponding all-electron data and all calculated values are in good agreement with experiment, apart from the usual over-binding behavior of LDA. The small differences between the results obtained by the two PPs and by the all-electron calculations suggest that our newly generated $Zn^{20+}/Ga^{21+}/In^{21+}$ PP (PP2) is of an acceptable accuracy.

The electronic structure and projected density of states (PDOS) for ZnX_2O_4 (X = Al, Ga and In) oxides, calculated using DFT/LDA, are shown in figure 1. $ZnAl_2O_4$ is direct band gap material with both the valence band maximum and the conduction band minimum at Γ, while $ZnGa_2O_4$ and $ZnIn_2O_4$ have an indirect band gap, as the valence band maximum is along the Γ–K direction (see inset). The PDOS shows a significant p–d hybridization between the Zn-d and O-p orbitals. This is one of the reasons why the DFT–LDA band gap of $ZnGa_2O_4$ is strongly underestimated compared to the experimental value as shown in table 2. The calculated band gap at the Γ point is 2.82 eV in comparison with the experimental value of 4.4–5.0 eV. The PDOS for $ZnAl_2O_4$ also shows p–d hybridization; however, the calculated band gap of 4.25 eV overshoots the experimental value of 3.8–3.9 eV. It is well known that DFT typically underestimates the band gap, as mentioned above, but it does so even more in the case of p–d hybridized systems. Thus the apparent band gap overestimation by DFT–LDA in the case of $ZnAl_2O_4$ is anomalous. Previous theoretical calculations on LDA level [5–7] found results similar to ours and have suggested that the experimental results require revision. In the case of $ZnIn_2O_4$, the DFT–LDA band gap is found to be 1.71 eV. No experimental information is available for comparison, as this material has not been synthesized experimentally.

The electron effective mass is listed in table 3 for ZnX_2O_4. The effective mass is calculated along the [111] direction, and it compares well to the known TCO materials such as ZnO (0.23 m_0) and In_2O_3:Sn (0.30 m_0). The effective mass with MBJ is larger than LDA, as also observed by Kim *et al* [27]. Another key property of a good TCO is a large second band gap between the two lowest conduction bands. The larger value of the second band gap lowers the

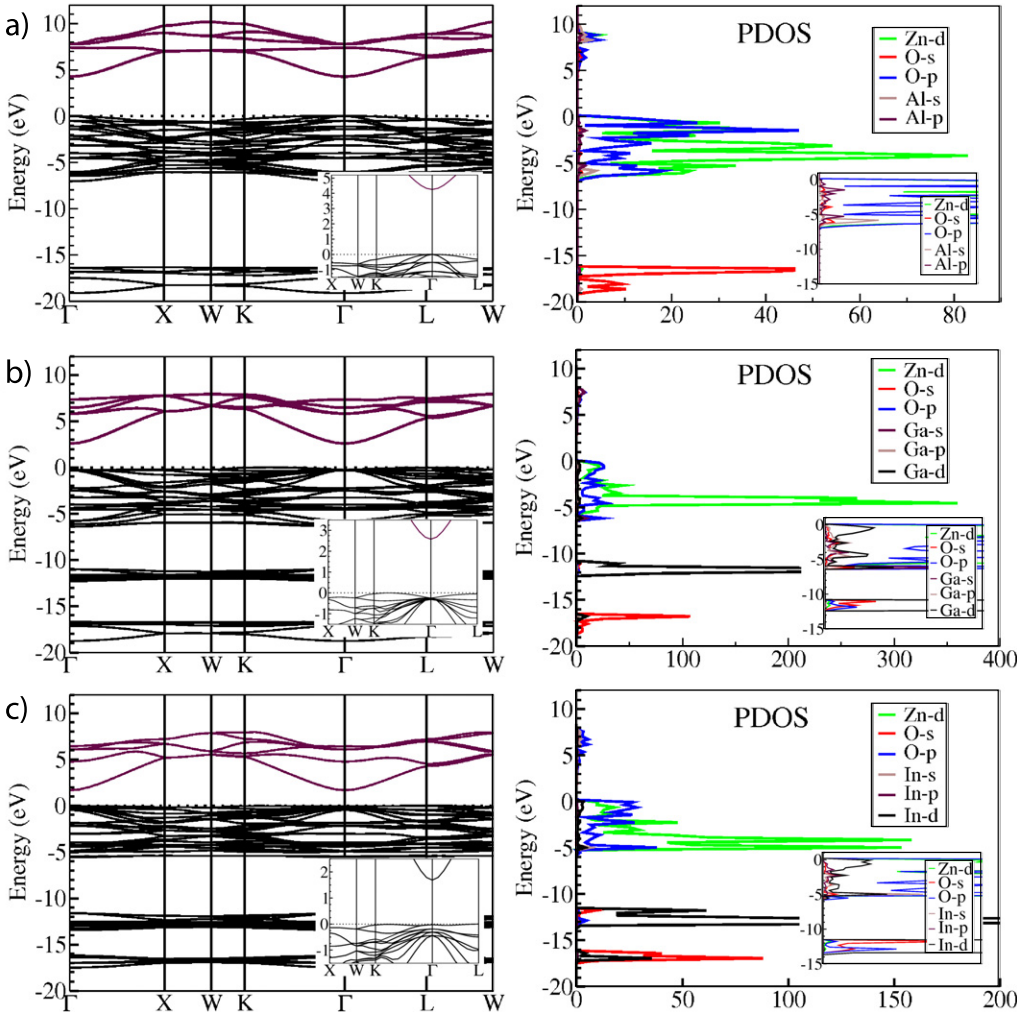

Figure 1. LDA (PP2) results on the electronic band structure and PDOS for (a) $ZnAl_2O_4$ (b) $ZnGa_2O_4$ and (c) $ZnIn_2O_4$ spinels.

Table 2. The DFT–LDA, all-electron, GW and MBJ band gap (E_g) at Γ, calculated with the optimized lattice constant (in eV).

Compound	E_g^{PP1}	E_g^{PP2}	E_g^{APW+lo}	E_g^{PP1+GW}	E_g^{PP2+GW}	E_g^{MBJ}	$E_g^{Expt.}$
$ZnAl_2O_4$	4.26	4.25	4.11	5.88	6.55	6.18	3.80–3.90
$ZnGa_2O_4$	2.63	2.82	2.53	3.88	4.57	4.71	4.40–5.00
$ZnIn_2O_4$	1.22	1.71	1.12	1.77	3.27	3.51	–

plasma frequency and results in reduced optical absorption [28]. We find that the second band gap (E_g^2) is 3.08 eV for $ZnAl_2O_4$, 3.10 eV for $ZnGa_2O_4$ and 3.13 eV for $ZnIn_2O_4$ with LDA. This shows that the ZnX_2O_4 spinels can be *n*-type conducting and remain transparent over the visible spectrum, making them attractive host materials for TCO.

Table 3. The electron effective mass (in units of free electron mass m_0), calculated along the [111] direction.

Compound	m_e^* (PP1)	m_e^* (APW + lo)	m_e^* (MBJ)
$ZnAl_2O_4$	0.37	0.35	0.44
$ZnGa_2O_4$	0.23	0.25	0.35
$ZnGa_2O_4$	0.17	0.22	0.34

To predict the band gap values accurately and to describe the conduction bands, we performed a calculation of the excited states using the GW approximation as well as the MBJ potential. Our findings are reported in the following sections.

3.2. GW and MBJ band gaps

We first calculate the quasiparticle correction to the band gap using the GW approximation. The Kohn–Sham(KS)-DFT band structure calculated with a norm-conserving PP serves as a starting point for the *ab initio* excited state calculation. The self-energy operator is calculated as $\Sigma = iGW$, where G is the one-particle Green function and W is the screened Coulomb interaction. The quasiparticle equation

$$[T + V_{\text{ext}}(\mathbf{r}) + V_{\text{H}}(\mathbf{r})]\Psi_i(\mathbf{r}) + \int dr' \Sigma(\mathbf{r}, \mathbf{r}'; \epsilon_i{}^{\text{qp}})\Psi_i(\mathbf{r}') = \epsilon_i{}^{\text{qp}}\Psi_i(\mathbf{r}') \tag{1}$$

is then solved to obtain the quasiparticle energies ϵ_i^{qp} and the wave functions Ψ_i. In the above expression, T is the kinetic energy operator and V_{ext} and V_{H} are the external potential and the Hartree potential, respectively. In practice, both the G and W operators are constructed within the quasiparticle approximation by using the KS wave functions Ψ_i and energies ϵ_i obtained by DFT calculations. In this work, the self-energy is calculated with the now well-known non-self-consistent G_0W_0 approximation [10], where G_0 is the electron Green function corresponding to the DFT eigenvalues and eigenfunctions

$$G_0(\mathbf{r}, \mathbf{r}'; \epsilon) = \lim_{\delta \to 0^+} \Sigma_i \frac{\Psi_i(\mathbf{r})\Psi_i^*(\mathbf{r}')}{\epsilon - [\epsilon_i + i\delta \text{sgn}(E_{\text{f}} - \epsilon_i)]}, \tag{2}$$

and W_0 is the dynamically screened Coulomb interaction

$$W_0(\mathbf{r}, \mathbf{r}'; \epsilon) = \int dr'' \varepsilon^{-1}(\mathbf{r}, \mathbf{r}''; \epsilon)\nu(\mathbf{r}'', \mathbf{r}'). \tag{3}$$

Here E_{f} is the Fermi energy, ν is the bare Coulomb interaction and ε^{-1} is the inverse dielectric matrix.

In the following, we present the quasiparticle band gaps obtained with the two sets of PPs (PP1 and PP2) for Zn, Ga and In (table 2). We discuss $ZnGa_2O_4$ first. The band gap with plain LDA is about 2.6 eV, with minor influences due to the type of PP or the use of an all-electron method. This gap is 2 eV below the experimental value. When the GW method is used for the standard PP (PP1), the resulting band gap is 1.2 eV larger. This is considerably closer to experiment, but still almost 1 eV too small. If, however, we use the Zn^{20+} and Ga^{21+} PP (PP2), we obtain a band gap of 4.57 eV, which agrees nicely with the experimental value. Hence, we confirm that similar to ZnO [16], the Zn^{20+} and Ga^{21+} PP (PP2) is essential for an

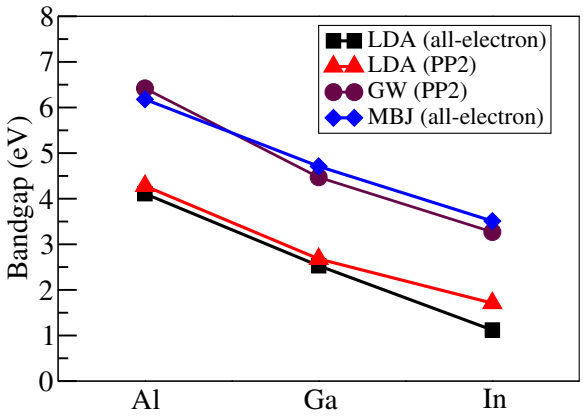

Figure 2. DFT–LDA, all-electron, GW and MBJ band gap of ZnX_2O_4 (X = Al, Ga and In) in spinel oxides.

adequate treatment of the self-energy. The MBJ band gap is similar to the GW (PP2) band gap. To elucidate the contribution of the Ga^{21+} PP to the self-energy, we now provide an interesting comparison. We have also calculated the GW band gap of $ZnGa_2O_4$ using a combination of Zn^{20+} and Ga^{13+} PP. The calculated GW band gap is 4.39 eV and the quasiparticle correction to the band gap is 1.54 eV, which is lower than 1.74 eV when the Zn^{20+} and Ga^{21+} PP is used. This confirms that PP2 should be used for both the cations, Zn and Ga.

For $ZnAl_2O_4$, the situation is somewhat different. As mentioned in section 3.1, the LDA band gap is larger than the experimental value, which is an anomalous situation. LDA is known to provide band gaps that are considerably too small for oxides. Indeed, applying GW with the standard PP (PP1) gives a 1.6 eV increase in the band gap. Using the Zn^{20+} and Al^{3+} PP (PP2) increases the band gap further by yet another 0.7 eV. The final value of 6.55 eV is somewhat larger than the MBJ value of 6.18 eV, and either of both is more than 2 eV larger than the reported experimental value. This strongly suggests that the experimental value is indeed incorrect, and a re-measurement is suggested.

$ZnIn_2O_4$ shows qualitatively similar behavior: using GW with the standard PP increases the band gap, whereas using PP2 rather than PP1 gives an additional increase. In contrast to the previous two compounds, the second step introduces the larger change. This is consistent with the observation that even at the LDA level the introduction of PP2 increased the band gap by 0.5 eV. The MBJ band gap is again similar to the GW+PP2 value.

As table 2 shows, the MBJ band gaps fall within a range of at most 7% from the GW band gaps (PP2). This is fair agreement considering the large difference with the plain LDA band gaps. Possible reasons for the GW–MBJ differences are the following: (a) the fact that both band gaps are determined at the equilibrium lattice parameter as predicted by the corresponding code (ABINIT/WIEN2k) at LDA level (table 1), (b) the direct influence of the PP on the band gap and (c) the fact that the GW band gaps are non-self-consistent values.

The band gap evolution in ZnX_2O_4 when X moves down the group (X = Al, Ga, In) is shown in figure 2. The DFT, GW and MBJ results show a similar trend. The band gap decreases with heavier cation substitution in the ZnX_2O_4 spinel oxide. Al has no d-states, while both Ga and In possess filled shallow core d-states that lie mainly around −12 eV in the valence band. However, note, from the PDOS shown in the insets of figure 1, that these d-states are also

Table 4. Reaction energies of ZnX_2O_4 (X = Al, Ga and In) spinel oxide.

Reaction	Reaction energy (eV)
$ZnO + Al_2O_3 \rightarrow ZnAl_2O_4$	−0.83
$ZnO + Ga_2O_3 \rightarrow ZnGa_2O_4$	−0.90
$ZnO + In_2O_3 \rightarrow ZnIn_2O_4$	+0.53

Table 5. Average bond lengths (Å) for the X-containing distorted oxygen octahedron in the spinel-type ZnX_2O_4 and the corundum-type X_2O_3. The data for the spinels stem from the calculations in this work. The corundum data are experimental values from [29–31].

Bond	ZnX_2O_4			X_2O_3		
	Al	Ga	In	Al	Ga	In
X–O	1.88	1.89	2.17	1.92	2.00	2.16
O–O	2.66	2.68	3.07	2.68	2.80	3.03

present in the region −5 to 0 eV in the valence band. This indicates that these d-states increase the coupling with the O-2p levels. Therefore, we suggest that the fundamental electronic band gap decreases through enhanced p–d coupling below the valence band while moving from Al to Ga. Since the In-d orbitals have larger spatial extension compared with the Ga-d orbital, the band gap decreases further when Ga is replaced by In.

3.3. Formation enthalpy

Experimentally the $ZnIn_2O_4$ spinel structure has not been observed and thus there are no experimental reports on the band gap of $ZnIn_2O_4$. To examine the stability of ZnX_2O_4 spinel oxides, we calculate the enthalpy of the following reaction with standard PP (PP1) at the LDA level:

$$ZnO + X_2O_3 \rightarrow ZnX_2O_4.$$

The enthalpy of the reaction is obtained by taking the difference between the total energies of the systems constituting the reaction. ZnO (wurtzite), α-Al_2O_3 (corundum), β-Ga_2O_3 and In_2O_3 (bixbyite) are all well-known compounds. The total energy of these compounds is calculated at optimized lattice parameters. The calculated enthalpy of this reaction is listed in table 4. The calculated enthalpies are −0.83 and −0.90 eV for $ZnAl_2O_4$ and $ZnGa_2O_4$, respectively, indicating that these spinel structures are stable. However, for $ZnIn_2O_4$ the reaction enthalpy is +0.53 eV, indicating that the formation of the $ZnIn_2O_4$ spinel structure is thermodynamically unfavorable. This appears to be correlated with the crystal geometry as explained below. The building block of the spinel structure is a distorted oxygen octahedron that contains one atom of element X. Table 5 shows how the average O–O distance and O–X distance for this octahedron depend on X: the bond lengths are almost identical for X = Al and X = Ga and increase by more than 10% for X = In. A similar octahedron appears in the corundum structure. The corresponding average bond lengths are given as well: there is a 5% increase when Al is replaced

by Ga and a more than 10% increase when Al is replaced by In. The latter agrees with the spinel case. The difference between corundum and spinel lies in the small bond lengths for the $ZnGa_2O_4$ spinel. Apparently such small bond lengths cannot be maintained for $ZnIn_2O_4$, which renders this crystal unstable.

4. Conclusions

We calculate the quasiparticle band gap with two sets of PPs for Zn, Ga and In. The quasiparticle corrections for ZnX_2O_4 (X = Al, Ga and In) are presented. Our results show that the Zn^{20+}, Ga^{21+} and Ga^{21+} PPs are essential to calculate the GW band gap. The calculated GW and MBJ band gaps for $ZnGa_2O_4$ are 4.57 and 4.71 eV, respectively. These band gap values agree well with the reported experimental values of 4.40–5.00 eV. The predicted GW and MBJ band gap for $ZnAl_2O_4$ are 6.55 and 6.18 eV, respectively. It will be of great interest to see if future experimental work confirms these values. The DFT (PP and all-electron), GW and MBJ band gaps for ZnX_2O_4 all show a similar trend: a band gap decrease upon substitution by a heavier cation. The MBJ band gaps are in agreement with the GW counterparts for these compounds, which corroborates the claim that MBJ provides accurate band gaps for only a small computational effort. The calculated formation enthalpy for the ZnX_2O_4 spinel oxide structure indicates that $ZnAl_2O_4$ and $ZnGa_2O_4$ are stable. However, the formation of the $ZnIn_2O_4$ spinel structure is unlikely, which is consistent with the fact that experimentally the $ZnIn_2O_4$ spinel structure has not been observed.

Acknowledgments

We thank the ETSF team at the Université Catholique de Louvain for stimulating discussions. We acknowledge financial support from the IWT-Vlaanderen through the ISIMADE project, the FWO-Vlaanderen through project number G.0191.08 and the BOF-NOI of the University of Antwerp.

References

[1] Sampath S K and Cordaro J F 1998 *J. Am. Ceram. Soc.* **81** 649
[2] Cordaro J F 1998 *Patent 5820669* Hughes Electronic Corporation, Los Angeles, CA
[3] Lee Y E, Norton D P, Budai J D and Wei Y 2001 *J. Appl. Phys.* **90** 3863
[4] Kawazoe H and Ueda K 1999 *J. Am. Ceram. Soc.* **82** 3330
[5] Karazhanov S Z and Ravindran P 2010 *J. Am. Ceram. Soc.* **93** 3335–41
[6] Sampath S K, Kanhere D G and Pandey R 1999 *J. Phys.: Condens. Matter* **11** 3635
[7] Bouhemadou A and Khenata R 2006 *Phys. Lett.* A **360** 339
[8] Hohenberg P and Kohn W 1964 *Phys. Rev.* **136** B684
[9] Kohn W and Sham L J 1965 *Phys. Rev.* **140** A1133
[10] Aulbur W G, Jönsson L and Wilkins J W 2000 *Solid State Phys.* **54** 1
[11] Tran F and Blaha P 2009 *Phys. Rev. Lett.* **102** 226401
[12] Tran F, Blaha P and Schwarz K 2007 *J. Phys.: Condens. Matter* **19** 196208
[13] van Schilfgaarde M, Kotani T and Faleev S 2006 *Phys. Rev. Lett.* **96** 226402
[14] Rinke P, Qteish A, Neugebauer J, Freysoldt C and Scheffler M 2005 *New J. Phys.* **7** 126
[15] Rohlfing M, Krüger P and Pollmann J 1995 *Phys. Rev. Lett.* **75** 3489

[16] Dixit H, Saniz R, Lamoen D and Partoens B 2010 *J. Phys.: Condens. Matter* **22** 125505
[17] Troullier N and Martins J L 1991 *Phys. Rev.* B **43** 1993
[18] Perdew J P and Zunger A 1981 *Phys. Rev.* B **23** 5048
[19] Gonze X *et al* 2002 *Comput. Mater. Sci.* **25** 478
[20] Gonze X *et al* 2005 *Z. Kristallogr.* **220** 558
[21] Bruneval F, Vast N and Reining L 2006 *Phys. Rev.* B **74** 045102
[22] Monkhorst H D and Pack J D 1976 *Phys. Rev.* B **13** 5188
[23] Hill R J, Graig J R and Gibbs G V 1979 *Phys. Chem. Miner.* **4** 317
[24] Wei S H and Zhang S B 2001 *Phys. Rev.* B **63** 45112
[25] Blaha P, Schwarz K, Madsen G K H, Kvasnicka D and Luitz J 2001 *WIEN2K: An Augmented Planewave + Local Orbitals Program for Calculating Crystal Properties* (Wien, Austria: Karlheinz Schwarz, Techn. Universität) ISBN 3-950131-1-2
[26] Cottenier S 2002 *Density Functional Theory and the Family of (L)APW-Methods: A Step-by-Step Introduction* (Leuven, Belgium: Instituut voor Kern- en Stralingsfysica, K.U.Leuven) ISBN 90-807215-1-4 (freely available from http://www.wien2k.at/reg user/textbooks)
[27] Kim Y S, Marsman M, Kresse G, Tran F and Blaha P 2010 *Phys. Rev.* B **82** 205212
[28] Mryasov O N and Freeman A J 2001 *Phys. Rev.* **64** 233111
[29] Newnham R E and de Haan Y M 1962 *Z. Kristallogr.* **117** 235
[30] Marezio M and Remeika J P 1967 *J. Chem. Phys.* **46** 1862
[31] Christensen A N and Broch N C 1967 *Acta Chem. Scand.* **21** 1046